

Links between different models for multifragmentation

S. Das Gupta, J. Pan, I. Kvasnikova and C. Gale

Physics Department, McGill University, Montréal, QC, H3A 2T8, Canada.

(August 6, 2017)

Abstract

We establish links between three different models for multifragmentation: the percolation model, the lattice gas model and the statistical multifragmentation model. There are remarkable similarities between the lattice gas model and the statistical multifragmentation model. For completeness, we also compare with a model based upon classical molecular dynamics which gives rather different results.

PACS numbers: 21.60.-n, 21.10.-k

arXiv:nucl-th/9607017v1 11 Jul 1996

I. INTRODUCTION

In this paper we establish relationships between three models commonly used for the theoretical treatment of nuclear multifragmentation. These are (1) the percolation model [1,2], (2) the lattice gas model [3,4] and (3) a class of models that we generically call the statistical multifragmentation model (SMFM) [5–7]. A great deal of work in the last approach has been done. A complete description can be found in Ref. [5] and we will essentially follow the SMFM model presented there. Both the percolation and statistical multifragmentation model have been used for years. The lattice gas model is of more recent origin and can actually bridge the gap between those two seemingly totally different approaches.

The connection between the percolation and the lattice gas model was already elaborated upon when the lattice gas model was introduced. It is included here for completeness. The main objective of the present paper is to point out that even though the lattice gas model and SMFM start off with two seemingly very different premises, there are many common features between the two models. Prompted by this similarity, we are driven to try and draw a $P - V$ diagram for the SMFM and to obtain the parameters of its critical behaviour, as for the lattice gas. We view this current work as mostly theoretical and we shall make only brief references to experimental results. For completeness we also make some comparisons with a classical molecular dynamics model that is in some use at the present time.

II. THE LATTICE GAS AND PERCOLATION MODELS

The lattice gas model has been described before [3,4]. For completeness we describe some of its features that are relevant for this work.

The lattice gas approach is viewed in our context as a modeling tool for the later stages of nucleus-nucleus collisions. For the case of n nucleons at this nuclear disassembly phase, the lattice gas theory consists of placing those n nucleons at N lattice sites where $N \geq n$ (when $N = n$ the nucleus is at its normal volume). Each lattice site can be populated by one nucleon or none. In the lattice gas model we can not squeeze the nucleus to lower than normal volume. Later we will see that this feature is common to the SMFM also. The ratio N/n is equal to ρ_0/ρ_f where ρ_0 is the normal nuclear density $=0.16 \text{ fm}^{-3}$ and ρ_f is the freeze out density. The ratio N/n is a parameter of the model and previously we have found that the value 2.54 provided a good fit with data [3]. Two nucleons in adjacent lattice sites will interact with each other. We have previously taken this interaction to be attractive and equal to ϵ , irrespective of whether it is between like particles (p-p and n-n) or between unlike particles (n-p interaction). We shall still adopt this argument for the time being but we shall later improve on this point. To generate an event we have to put nucleons in sites at a given temperature, taking into account that it is energetically preferable to put a nucleon adjacent to an occupied site rather than adjacent to an empty one. This Monte-Carlo sampling involves a Hamiltonian and is more involved than in a pure site percolation model. As can be readily guessed, the temperature is related to the excitation energy per nucleon. Once the nucleons have been placed in lattice sites we have to specify the momentum of each nucleon. The momentum of each nucleon is generated by a Monte-Carlo sampling of a Maxwell-Boltzmann distribution for the specified temperature. Thus at a given temperature we can generate an event in which the potential energy is obtained from the number of $n - n$

bonds and the total kinetic energy is simply the sum of kinetic energies of the n nucleons. We now recall how clusters are generated in the model. Once we have put in the nucleons in their lattice sites and generated their momenta it is easy to calculate the cluster distribution. Two nucleons in adjacent sites will form a cluster or be part of the same cluster if the relative kinetic energy of the two nucleons is insufficient to overcome the attraction: $p_r^2/2\mu + \epsilon < 0$. Here μ is the reduced mass, and ϵ is a binding energy parameter from which the binding energy per nucleon can be calculated. Using this prescription, clusters in each simulation are easily found. It is also clear that in general, clusters do not have to appear in their ground state. They can be in an excited state. A comparison of yields of clusters calculated with this prescription was found in good agreement with many experiments [8,9]. Since the lattice gas model has a Hamiltonian, it is possible in principle to obtain an equation of state. The $P - V$ diagram for the lattice gas model was drawn in [4] for an infinite system using the Bragg-Williams approximation. Results from improved Bethe-Peierls approximation were also shown. Clear indications of thermal critical phenomena are seen. It will be useful to remember here that the $P - V$ diagram for lattice gas in the mean field approximation is similar to that of a Van der Waals gas. Improved calculations put the critical temperature at $1.1275|\epsilon|$. The critical density is $\rho_0/2$ [10].

The similarities of the lattice gas model with the percolation model are easy to see. For the latter we restrict ourselves to bond percolation model which is normally used for comparison with experiments. In terms of observables in heavy ion reactions, the bond percolation model is almost identical with the lattice gas model in the limit $N = n$. In the lattice gas model two nearest neighbours are bound to each other if $p_r^2/2\mu + \epsilon < 0$. This probability decreases with increasing temperature. In the bond percolation model the probability that bonds between nearest neighbours operate is given by a probability p which similarly decreases with increasing temperature. Indeed it was shown that the phenomenological parametrization for p used in bond percolation calculation makes the bonding probability same in both the models [11]. For a certain value of p , a critical percolation cluster will appear. In a bond percolation model there is a concept of temperature but the volume is not a variable. Thus the concept of pressure is also absent. This is still a very valuable model since the fragment distribution, which is the experimental observable, is dictated by percolation characteristics. It is evident that the lattice gas model possesses the percolation model as a subset. In addition to containing all the percolation phenomena not only at normal volume but also at larger volumes, it also has thermal phase transitions. The concepts of temperature, pressure and volume are all valid concepts. An equation of state curve can be drawn for the lattice gas model but the percolation model is missing a parameter and we can not thus plot a traditional equation of state.

III. THE STATISTICAL MULTIFRAGMENTATION MODEL

Our arguments follow those presented in Ref. [5] except that since we are not as much interested in comparing with data as with connections between different models, we will make some simplifications. One assumes that equilibration has taken place in a freeze-out volume which is greater than normal nuclear volume. In this volume composites of different mass numbers appear. The volume of any of these composites will be its normal nuclear volume, i.e., k/ρ_0 where k is the mass number of the composite. It then follows that if the

total number of nucleons that are fragmenting is n , the excluded volume V_{ex} is n/ρ_0 and the available volume for thermalization is $V_f = V - V_{ex}$. The concept of excluded volume is also present in the lattice gas model. Apart from the excluded volume the lattice gas model has a potential, as evidenced by the attraction ϵ between nearest neighbour nucleons. This results in binding energy for each cluster. In the SMFM the specific two body interaction is not written down but there is clearly a potential energy and it makes its presence felt through the explicit binding energy of clusters. In the SMFM the clusters can be in excited states. In the lattice gas model also the clusters can be in excited states (excited states are not necessarily included in the same fashion in both models but provisions are kept for their inclusion). Surface tension is included in the SMFM in the binding energy relation for clusters (see below). This appears naturally in the lattice gas model as nucleons at the edge of a cluster will see an anisotropic neighbour distribution. It is because of interactions that the multiplicity changes in the SMFM when either the temperature or the density varies. The potential energy will also change with density. We therefore postulate that we have an interacting system where interactions lead to clusters with associated binding energy. Because of the short range of the interactions two different clusters do not interact except through the excluded volume effect. We can then apply the law of partial pressures to obtain an equation of state.

IV. THE EQUATION OF STATE IN THE SMFM

For a given freeze-out volume and temperature we can have n_1 nucleons, n_2 clusters of size 2, n_3 clusters of size 3, etc. . . An extraordinarily large number of choices are possible and the most probable distribution is obtained for that choice of $n_1, n_2, n_3 \dots$ such that the free energy is minimized. We take this most probable distribution as the appropriate distribution for the calculation of pressure. Following the work of Ref. [5], the number of clusters of size k in volume V_f is given by

$$n_k = \exp [k\beta\mu] \frac{V_f}{h^3} (2\pi mT)^{3/2} k^{3/2} \exp [\beta F(k)] , \quad (4.1)$$

where m =mass of a nucleon, $F(1) = 0$ and for $k > 1$

$$F(k) = (Wk - \sigma(T)k^{2/3}) - \langle E^* \rangle + TS \quad (4.2)$$

where $W = 16$ MeV is the volume energy term, $\sigma(T)k^{2/3}$ gives the surface tension correction, $\langle E^* \rangle = \pi^2 T^2 / (4\epsilon_F)$ is the average excitation energy for the composite and S , the entropy, is $S = \pi^2 T / (2\epsilon_F)$. For the numerical work, we use $(4/\pi^2)\epsilon_F = 16$ MeV. The chemical potential μ in Eq. (4.1) is fixed from the condition $\sum_1^n kn_k = n$. The pressure is calculated from $P(\rho, T) = T/V_f(\sum n_k)$. Here $\rho = n/(V_f + V_{ex})$. In the above we have used the grand canonical ensemble. The surface tension $\sigma(T)$ is taken as a function of temperature [5]. For the discussion to follow the surface tension plays a crucial role. The SMFM-as the lattice gas type models-is capable of producing a U shaped distribution for $Y(Z)$, the fragment yield function, against Z , the fragment charge. This would not be possible without the surface tension term. We also studied a SMFM model in which surface tension is not a function of temperature. The major features do not change in what we describe below.

The $P - \rho$ diagrams using this formalism were done for $A = 85$ [8], and also for $A = 137$ (and $Z = 57$), a fragment size roughly corresponding to the projectile fragmentation of a gold nucleus. In Figs. 1 and 2 we have shown the case of $A = 137$. The $P - \rho$ diagram of Fig. 1 is strongly suggestive of a liquid- gas type phase transition. Isotherms at $T = 5$ and 6 MeV show regions where pressure is very flat, over large variations of ρ . A totally constant value of P against ρ in some region implies that isothermal compressibility $\kappa = 1/\rho(\partial\rho/\partial P)_T$ goes to infinity as will happen if one moves along the Maxwell construction for a Van der Waals gas. This flat region disappears above the critical point. Above the critical point the compressibility is a monotonically decreasing function of density. In Fig. 1, the pressure against ρ is not strictly constant in the mixed region but has a slight rise. Thus the compressibility is not infinite but reaches a maximum. This is sensible: infinities will get replaced by maxima in a finite system. We identify the critical point by the disappearance of the maximum in κ (Fig. 2). For a system of mass 137 we estimate $T_c = 6.8$ MeV and $\rho_c = 0.4\rho_0$. For a system of 85 particles the same criteria gave $T_c = 6.2$ MeV and $\rho_c = 0.14\rho_0$. Values of critical temperature and density for mass number 137 are not a great deal different from what is obtained in the lattice gas model for an infinite system. A binding energy of 16 MeV in nuclear matter requires a value $\epsilon = -5.33$ MeV. The parameters of the critical point in the lattice gas model will then be $T_c = 6.0$ MeV and $\rho_c = \rho_0/2$.

V. THE EQUATION OF STATE IN THE LATTICE GAS MODEL

We would like to draw $P - V$ diagrams similar to above using the lattice gas model. Unfortunately, this is prohibitively difficult. While energy, fluctuations in energy (essentially C_v) and several other quantities can be obtained using Monte-Carlo simulations (later we will show results of such calculations) calculation of pressure requires evaluation of the partition function which can not be done using Monte-Carlo. We can draw a $P - V$ diagram using mean field theory (this was already done in Refs. [3,4]) but this has in some part of the diagram a wrong slope of pressure against ρ (in fact one uses that as a signature of phase-transition) and does not compare well with fig. 1.

While better calculations for pressure are possible, for a limited comparison we do the following calculation. We use a lattice of 3^3 (this approach can not be improved by a straightforward increase of lattice dimensions: computation with a 4^3 lattice will take 2^{37} times as much time and is clearly beyond our scope) but use periodic boundary conditions to minimize edge and finite particle number effects [12]. This represents an improvement over the Bethe-Peierls calculation done in Ref. [4], as our lattice is in fact much larger than a Bethe-Peierls block. We use $PV = T \ln Z_{gr}$, where the grand partition function is $Z_{gr} = \sum_0^{27} e^{\lambda n} Z(n)$. The value of λ is chosen to give the required value of $\rho/\rho_0 = \langle n \rangle / 27$ where $\langle n \rangle = \partial \ln Z_{gr} / \partial \lambda$. Finally $V = 27a^3$ where $a^3 = 1.0/\rho_0$. In figures 3 and 4 we have plotted $p - V$ and $\kappa - \rho$ diagram. Similarities with Figs. 1 and 2 are obvious. A critical temperature between 5 and 6 MeV is suggested but one should keep in mind the limitations induced by the smallness of the lattice. The value of ϵ used for these diagrams was -5 MeV.

VI. SPECIFIC HEAT

The simple SMFM model as used here gives a maximum in C_v as one moves across T_c along a density close to the critical density. This is shown in Fig. 5. This of course is in keeping with the findings of previous detailed investigations [7,13]. Similar maxima in C_v are found also in the lattice gas model. We will show our results for $n=137$ which roughly corresponds to the projectile fragmentation of gold in the EOS TPC experiment. The lattice sizes are taken to be $N = 7^3$ and $N = 8^3$ which would correspond to two different freeze-out densities. For this calculation we use Monte-Carlo sampling based upon the Metropolis algorithm. At a given temperature we generate an event in which the potential energy is obtained from the number of nucleon-nucleon bonds and where the kinetic energy is simply the sum of kinetic energies of the nucleons. The average of many such events gives the average energy per nucleon, e , at a given temperature. One can then obtain C_v per nucleon by numerically differentiating $\partial e/\partial T$ or else, since the events are generated in the canonical ensemble in the Metropolis algorithm, one can use

$$C_v = \frac{1}{nT^2}(\langle E^2 \rangle - \langle E \rangle^2). \quad (6.1)$$

Note that $\langle E \rangle = en$.

We use this opportunity to introduce an improvement to the lattice gas model. In our previous work we used the same value of ϵ for attraction between like (nn and pp) and unlike (np) particles. Although this already gives a rather reasonable overall fit to $Y(Z)$ against Z one gets a theory with di-neutrons di-protons etc... This can be avoided by postulating two kinds of bonds: that between the proton and the neutron which we denote as ϵ_{np} and is attractive, and that between identical particles (neutron-neutron and proton-proton) which we denote by ϵ_{nn} and which is either zero or repulsive. In accordance with a molecular dynamics potential [14] which we will refer to in the next section we have used a slightly repulsive interaction for $\epsilon_{nn} = 1$ MeV. The attractive interaction is set at $\epsilon_{np} = -5$ MeV

In each Monte-Carlo simulation we also obtain the cluster decomposition. After a large number of simulation one obtains $Y(Z)$ against Z . We expect that near the critical point a power law will emerge : $Y(Z) \propto Z^{-\tau}$. The exponent τ will be minimum at the critical point. We deduce an effective value of τ from our simulation even when far from the critical point by using the formula [15]:

$$\frac{\sum_2^{10} ZY(Z)}{\sum_2^{10} Y(Z)} = \frac{\sum_2^{10} ZZ^{-\tau}}{\sum_2^{10} Z^{-\tau}} \quad (6.2)$$

The variation of τ against the temperature is shown in Fig. 6. The calculated C_v against temperature is shown in Fig. 7. We find that the maximum in the value of the specific heat happens at the same temperature where the value of τ minimizes. In so far as the C_v maximizes at the critical temperature, the prediction of the lattice gas model is similar to that of SMFM. We also note that using different bonds between like and unlike particles (which is more realistic than the simpler case) actually enhances the peak.

In detail the calculated values of C_v 's differ, specially at low temperature. Here the SMFM is clearly more realistic. At low temperature, the breakup event will have one large cluster and the specific heat of this cluster will dominate the net contribution. In SMFM the

low energy excitation energy characteristics is put in by hand and hence C_v has been forced to go like T . In the lattice gas model the low temperature value of the specific heat per particle will simply be $3/2$. This comes from the classical simulation of the kinetic energy of the constituent nucleons. Stated another way, the excited states of each cluster is put in differently in the two models.

One can use the lattice gas model for predicting a caloric curve (temperature plotted against excitation energy), provided one assumes that calculations using the lattice gas model are valid beyond a certain temperature only. The uncertainty below this temperature can be absorbed in one constant. In Fig. 7 we show a caloric curve obtained in the lattice gas model. In the figure we also show a comparison with experimental data. To produce the caloric curve we use

$$e(T) = \int_0^t C_v dT' + \int_t^T C_v dT' = \varepsilon + \int_t^T C_v dT' \quad (6.3)$$

We ignore the prediction of the lattice gas model below a temperature t (taken in this work to be 3.2 MeV) and we thus introduce a parameter ε . The caloric curve beyond the temperature 3.2 MeV is shown in Fig. 8. In the ALADIN results [16], T against the excitation energy is considerably flatter at temperature around 5 MeV, implying a large increase in the value of the specific heat at this temperature. We do not get such a large value of C_v in our calculations. The appearance of a possible plateau in the caloric curve is also less dramatic in the recent EOS TPC data [17].

We end this section by summarizing the comparison between the lattice gas model and SMFM. As we have shown there are many common features in the two models. The lattice gas model has the advantage of having considerable recognition in statistical physics. It defines a two body interaction which is used for all its predictions. Phase transitions in the model are well-studied and well-defined. Another advantage is that fragment formation in non-spherical geometries can be studied. Such geometries do occur in heavy-ion collisions [18]. The advantage of SMFM type models is that binding energy, surface tension and excited states can all be inputs in the model. This makes accurate comparison with experiments more feasible. No detailed theory of phase transitions in this type of models has yet been completed. It is not clear how non-spherical geometries might influence the results.

For completeness, we now turn to a discussion of how classical molecular dynamics predictions differ from those of the previous approaches.

VII. NUCLEAR PROPERTIES IN CLASSICAL MOLECULAR DYNAMICS

Here, we choose to study equilibrium properties of nuclear systems using the methods of classical molecular dynamics. Our first task is to specify the nucleon-nucleon interaction. We use a neutron-proton interaction, $v_{np}(\mathbf{r})$, which is attractive for large values of the separation distance \mathbf{r} , but repulsive for small values. The like-particle nuclear potentials, v_{nn} and v_{pp} are taken to be identical and purely repulsive. Those features are chosen to satisfy the basic requirements of nuclear phenomenology. Our interparticle nuclear potentials are given as a combination of Yukawa interactions [14]:

$$v_{nn}(\mathbf{r} < \mathbf{r}_c) = v_0 [\exp(-\mu_0 \mathbf{r})/\mathbf{r} - \exp(-\mu_0 \mathbf{r}_c)/\mathbf{r}_c] , \quad (7.1)$$

$$v_{\text{np}}(\mathbf{r} < \mathbf{r}_c) = v_r [\exp(-\mu_r \mathbf{r})/\mathbf{r} - \exp(-\mu_r \mathbf{r}_c)/\mathbf{r}_c] - v_a [\exp(-\mu_a \mathbf{r})/\mathbf{r} - \exp(-\mu_a \mathbf{r}_c)/\mathbf{r}_c] . \quad (7.2)$$

In the above, \mathbf{r}_c is fixed at 5.4 fm, a simple and adequate cutoff. It is also implied that

$$v_{\text{nn}}(\mathbf{r} \geq \mathbf{r}_c) = v_{\text{pp}}(\mathbf{r} \geq \mathbf{r}_c) = 0 . \quad (7.3)$$

The parameters of the potentials are $v_0 = 373.118$ MeV fm, $v_r = 3088.118$ MeV fm, $v_a = 2666.647$ MeV fm, $\mu_0 = 1.5$ fm⁻¹, $\mu_r = 1.7468$ fm⁻¹, and $\mu_a = 1.6$ fm⁻¹. The nuclear compressibility coefficient, K , is 250 MeV for this choice of parameters [14]. In the case of proton-proton interactions, the Coulomb interaction can be added separately. However, in order to make a consistent comparison, the Coulomb effects were left out in this work.

In the molecular dynamics simulation, the particles are propagated in phase space by integrating Newton's equations of motion through a "leap-frog" algorithm [19]. Because we shall address shortly the issue of specific heat, we chose to perform simulation of canonical ensembles. One can show [19] that constant temperature dynamics are generated by the following equations of motion for the position \mathbf{r}_i and the momentum \mathbf{p}_i of each individual particle i of mass m subject to a force \mathbf{f}_i :

$$\dot{\mathbf{r}}_i = \mathbf{p}_i/m \quad (7.4)$$

$$\dot{\mathbf{p}}_i = \mathbf{f}_i - \xi \mathbf{p}_i \quad (7.5)$$

The quantity ξ acts as a "friction coefficient" that is recalculated at each time step and keeps the temperature constant to a high level of precision [20]. The system is initialized in momentum space from a Monte Carlo sampling of a Boltzmann distribution, and then cooled to the desired temperature. This method ensures a proper thermodynamic equilibrium distribution for the nucleons in interaction. The nucleons are confined to box whose volume is adjusted to yield the desired density.

In our canonical ensemble simulations, the pressure can then be calculated for a system of n interacting nucleons by means of a virial expansion [21]:

$$\frac{P_{\text{virial}}}{\rho T} = 1 - \frac{1}{6nT} \left\langle \sum_i \sum_{j>i} r_{ij} \frac{\delta v_{ij}}{\delta r_{ij}} \right\rangle . \quad (7.6)$$

Note that we are using units where the Boltzmann constant, k_B , is unity. The potential energy between two nucleons i and j , separated by a distance r_{ij} , is written as v_{ij} . It is straightforward to calculate the average total energy and the average total energy squared, so that the specific heat, C_v , can easily be inferred from Eq. (6.1). Note that microcanonical molecular dynamics has been used in the recent past to study the multifragmentation behaviour of heavy ion systems [22,15].

On Fig. 9 we plot pressure isotherms obtained in molecular dynamics of our nuclear fluid with the potential of Eq. (7.2), for a system of $A = 137$ and $Z = 57$. We restrict our calculation to the range of temperatures and densities related to this comparative study with the lattice gas model and SMFM. In this temperature range, one realizes that the molecular dynamics predictions are devoid of the plateau regions characteristic of the above two approaches. It appears that the critical behaviour of the molecular dynamics ensembles

is in fact at a temperature just below 1 MeV and at nuclear densities around $\approx \rho_0/3$. Those parameters follow from our own simulations [20] and are also in line with those found in a similar effort, using however a slightly different potential [15]. Turning to the calculations of C_v plotted on Fig 10, we come to conclusions similar to the ones reached in our study of the equation of state, namely that the specific heat does not exhibit any striking behaviour. There are no noticeable peaks that would follow from a flattening of the caloric curve, at the temperatures and densities dictated by our comparative study. At high temperatures, C_v tends to its value for noninteracting gases: $C_v = 3/2$. We will not insist further here on a detailed molecular dynamics study of the thermodynamic properties of the nuclear fluid at finite temperatures, as this does not pertain directly to the work at hand. This is however done and will appear elsewhere [20].

VIII. CONCLUSIONS

We have shown that some popular theoretical approaches to nuclear multifragmentation shared several common features. Those models are the percolation, lattice gas and statistical multifragmentation. The connection between the lattice gas and percolation models is more apparent and has been pointed out before, but two models that previously appeared rather unrelated, the lattice gas and SMFM, have some remarkable similarities to each other. We see this point as being quite important, as it represents a rather satisfying unity aspect from a theoretical perspective. This is the aspect we chose to insist on in this work.

We also have shown some comparisons with calculations done in a classical molecular dynamics scenario. The results there are quite different. There are of course obvious deficiencies associated with the use of a classical approach to a system in a regime where the quantum aspects are undoubtedly important. We plan to investigate those deficiencies, and their effects, further.

IX. ACKNOWLEDGEMENTS

Our research is supported in part by the Natural Sciences and Engineering Research Council of Canada and in part by the Fonds FCAR of the Québec Government.

REFERENCES

- [1] W. Bauer, Phys. Rev C **38**, 1297 (1988).
- [2] X. Campi, Phys. Lett. **B 208**, 351 (1988).
- [3] J. Pan and S. Das Gupta, Phys. Lett. **B 344** 29 (1995).
- [4] J. Pan and S. Das Gupta, Phys. Rev. C **51**, 1384 (1995).
- [5] J. P. Bondorf, A. S. Botvina, A. S. Ijilinov, I. N. Mishustin, and K. Sneppen, Phys. Rep. **257**, 133 (1995), and references therein.
- [6] G. Fai and J. Randrup, Nucl. Phys. **A 381**, 557 (1982).
- [7] B. H. Sa and D. H. E. Gross, Nucl. Phys. **A 437**, 643 (1985).
- [8] T. Li et. al., Phys. Rev. Lett. **70**, 1924 (1993).
- [9] L. Beaulieu et. al., submitted for publication.
- [10] R. B. Stinchcombe, *Phase Transitions and Critical Phenomena*, vol. 7, eds. C. Domb and J. L. Lebowitz, Academic Press, London (1983).
- [11] S. Das Gupta and J. Pan, Phys. Rev C **53**, 1319 (1996).
- [12] J. J. Binney, N. J. Dowrick, A. J. Fisher, and M. E. J. Newman, *The theory of critical phenomena*, Oxford University Press, Oxford (1993).
- [13] J. Bondorf, R. Donangelo, I. N. Mishustin and H. Schulz, Nucl. Phys **A 444**, 460 (1985).
- [14] R. J. Lenk, T. J. Schlagel, and V. R. Pandharipande, Phys. Rev. C **42**, 372 (1990).
- [15] S. Pratt, C. Montoya, and F Ronning, Phys. Lett. **B 349**, 261 (1995).
- [16] J. Pochodzalla et. al., Phys. Rev. Lett. **75**, 1040 (1995).
- [17] A. Hirsch, private communication.
- [18] L. Phair, W. Bauer, and C. K. Gelbke, Phys. Lett. **B 314**, 271 (1993).
- [19] See, for example, M. P. Allen and D. J. Tildesley, *Computer Simulations of Liquids*, Oxford University Press, Oxford (1987).
- [20] I. Kvasnikova, MSc thesis, McGill University (1996).
- [21] J. R. Waldram, *The Theory of Thermodynamics*, Cambridge University Press, Cambridge (1985).
- [22] V. Latora, A. Del Zoppo and A. Bonasera, Nucl. Phys. **A 572**, 477 (1994); P. Finocchiario, M. Belkacem, T. Kubo, V. Latora and A. Bonasera, nucl-th/9512019.

FIGURES

FIG. 1. A plot of pressure against ρ/ρ_0 for the SMFM used in this work. The flat parts for the 5 and 6 MeV isotherms signify mixed phases.

FIG. 2. The compressibility $\kappa = 1/\rho(\partial\rho/\partial P)$ at constant temperature for temperatures in the vicinity of the critical temperature. The maximum disappears at T_c .

FIG. 3. The $P - \rho$ diagram from the lattice gas model obtained by using a 3^3 lattice and imposing periodic boundary conditions.

FIG. 4. The isothermal compressibility κ at various temperatures for the 3^3 lattice.

FIG. 5. The specific heat per particle for the SMFM used in the text for a system of 137 nucleons. Two different freeze-out densities are used. The specific heat is dimensionless here as the unit for both heat and temperature is MeV.

FIG. 6. The exponent τ calculated in the lattice gas model for a system of 137 particles. We show results when the same value of ϵ is used for like and unlike particles and also when they are different. In the latter case we show results for two densities.

FIG. 7. The specific heat per particle in the lattice gas model for a system of 137 particles. The maxima here closely coincide with the positions of the minima in Fig. 6.

FIG. 8. The caloric curve calculated according to lattice gas model for a system of 137 particles and compared with ALADIN data (data set II), Ref. [16] and with EOS TPC data (data set I), Ref. [17].

FIG. 9. Pressure isotherms calculated in classical molecular dynamics, for temperatures ranging from 1 to 4 MeV. We limit ourselves to densities lower than the equilibrium nuclear matter density, ρ_0 . The error bars are not shown. The errors are negligible below $\rho/\rho_0 \approx 0.5$, and slowly rise to be $\approx 5\%$ near $\rho/\rho_0 = 1$.

FIG. 10. The specific heat per nucleon, C_v , calculated in classical molecular dynamics. Three representative values of nuclear density are shown. The errors are statistical.

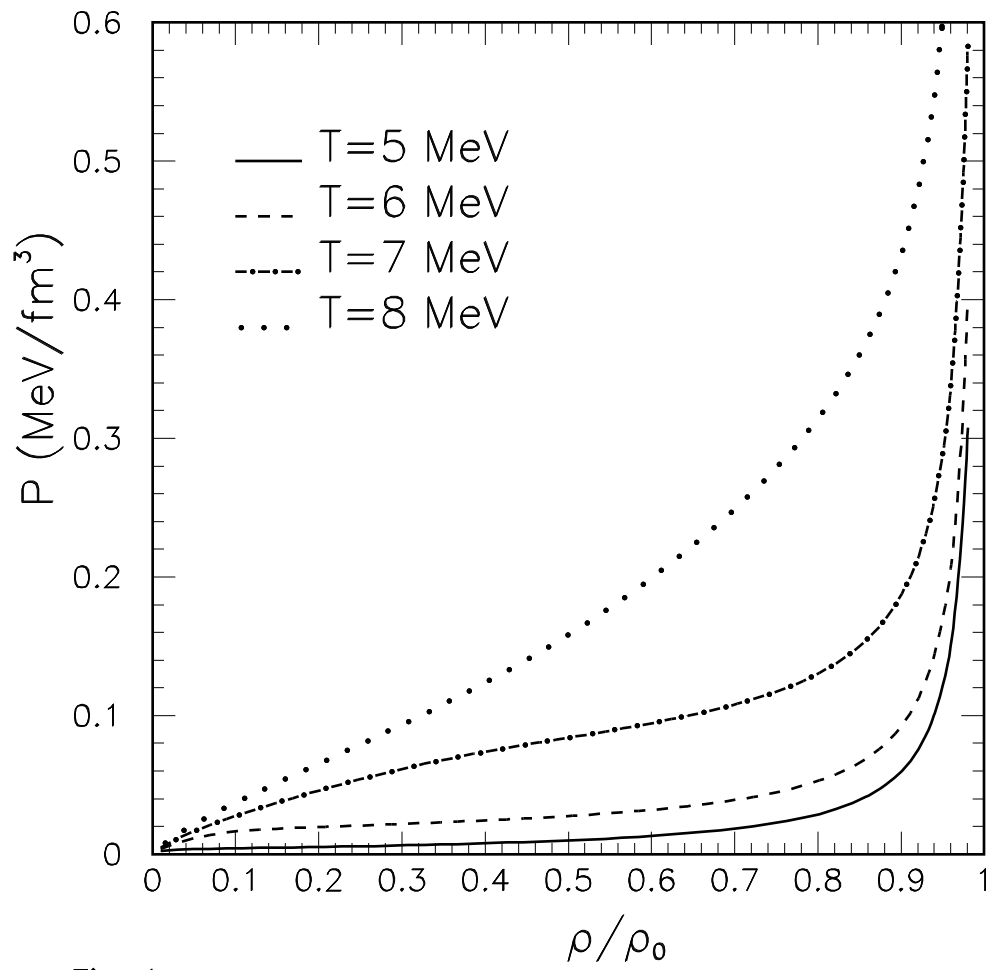


Fig. 1

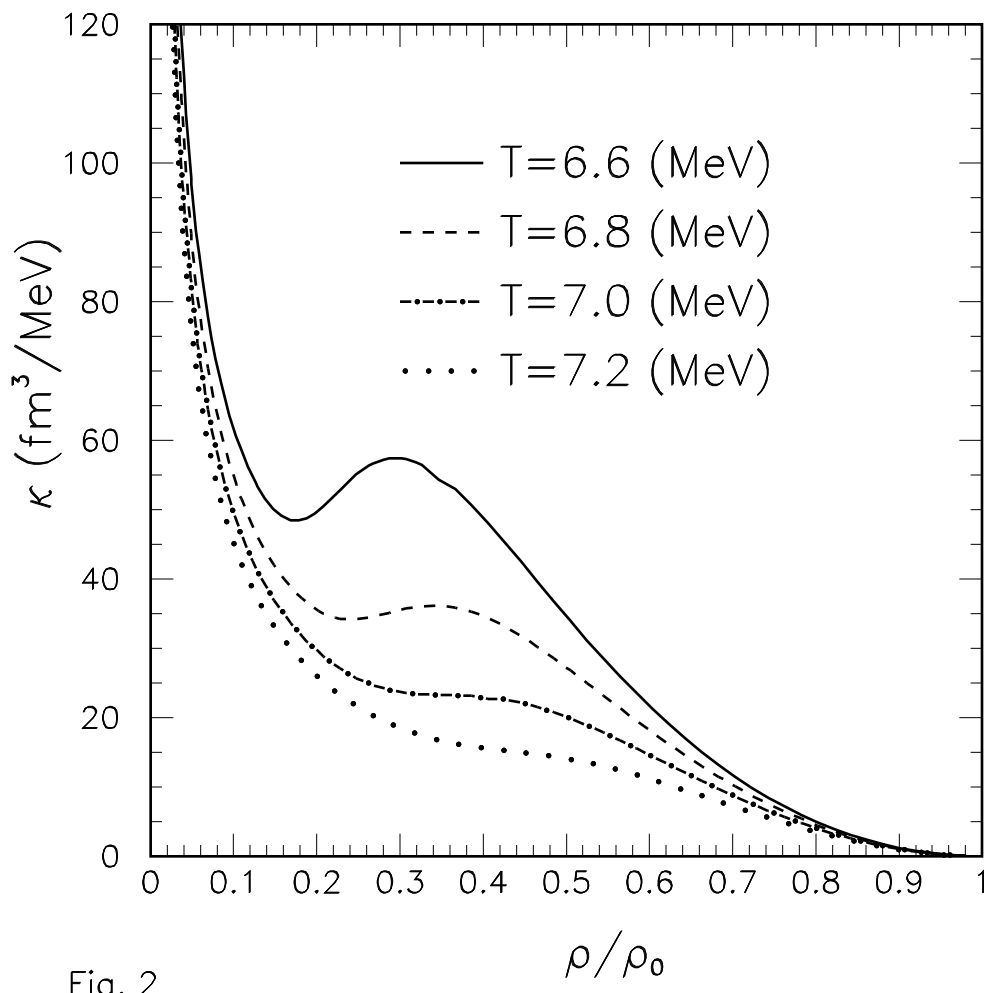


Fig. 2

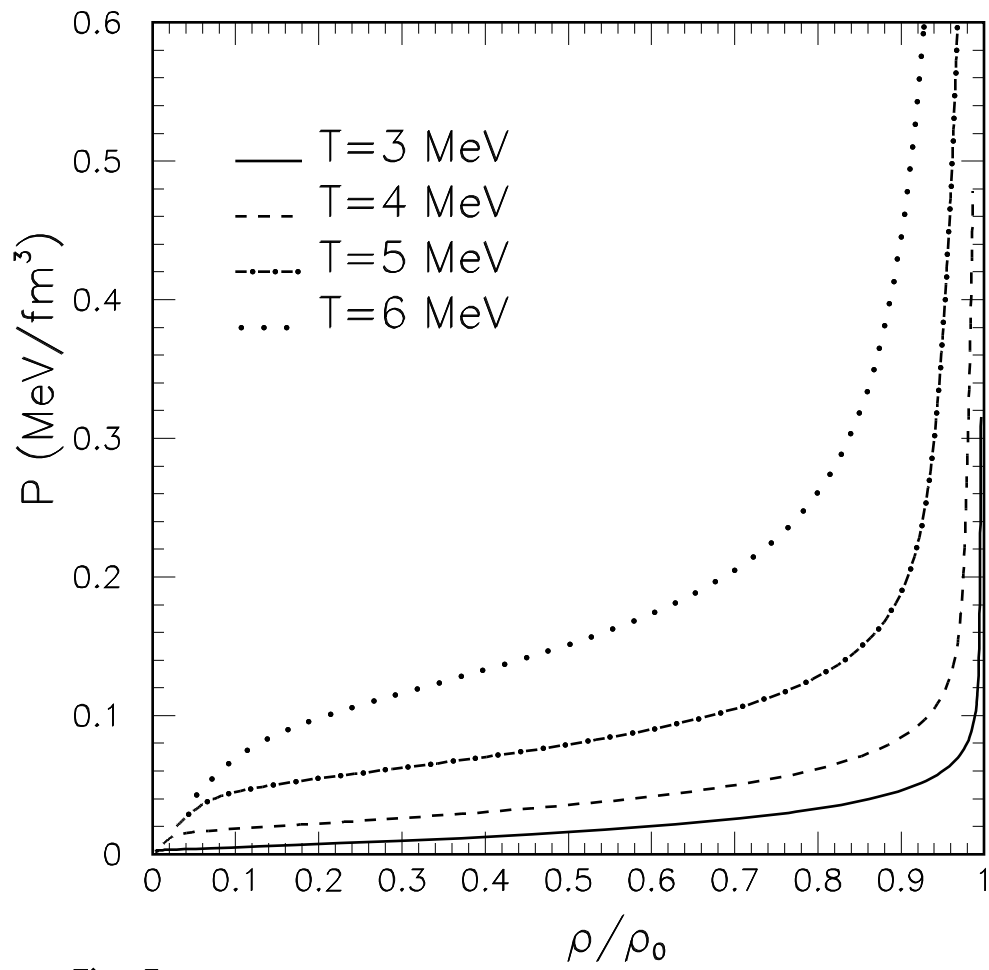


Fig. 3

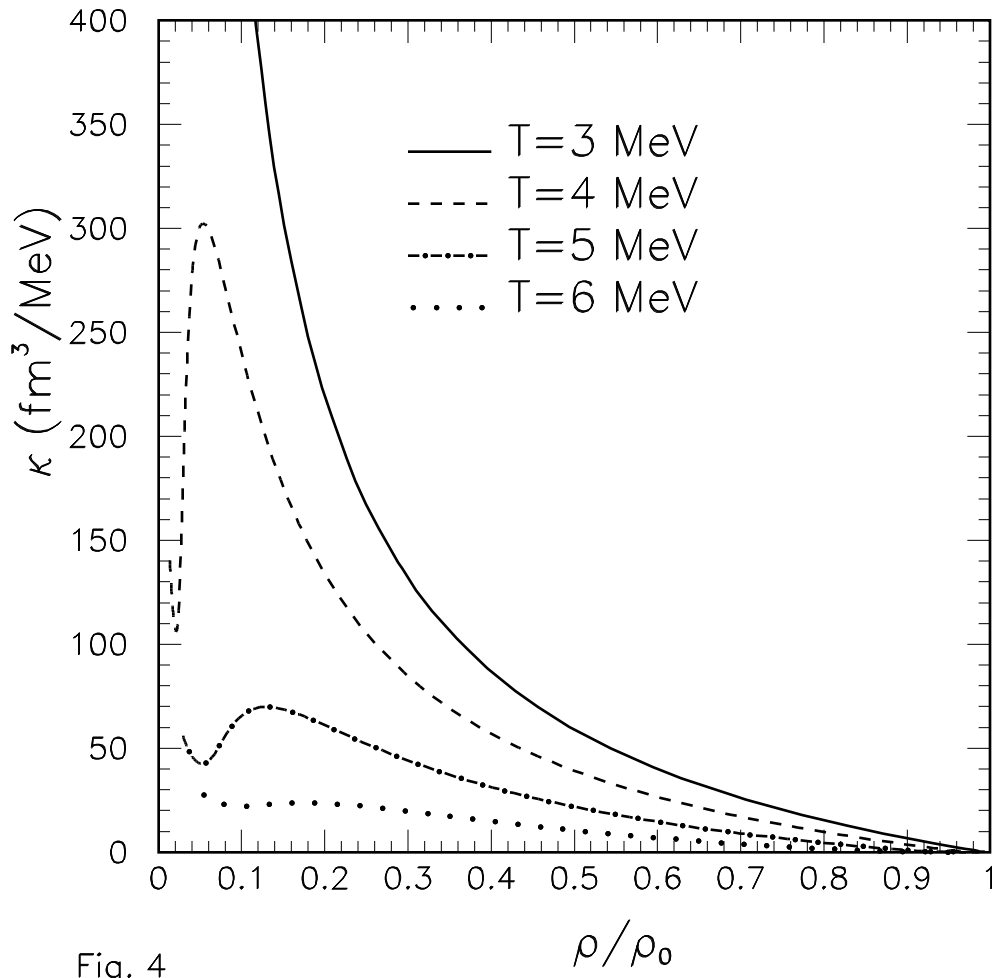


Fig. 4

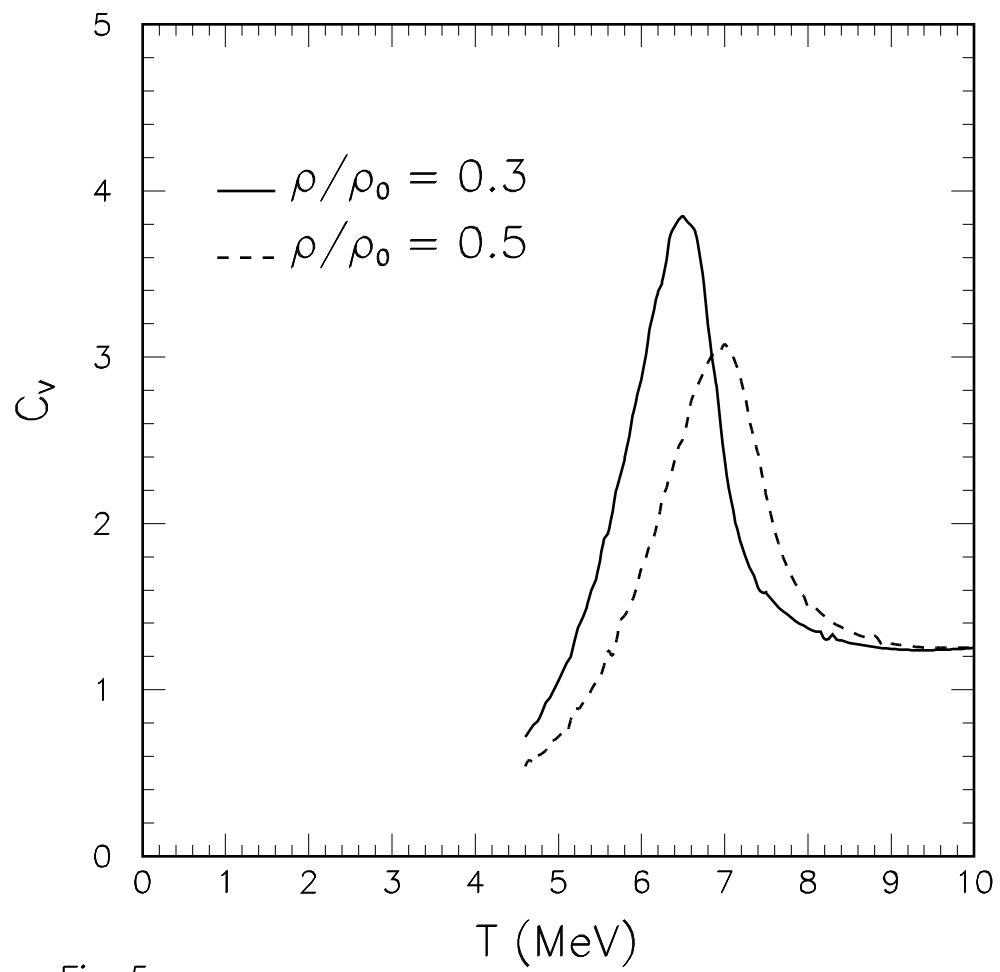


Fig. 5

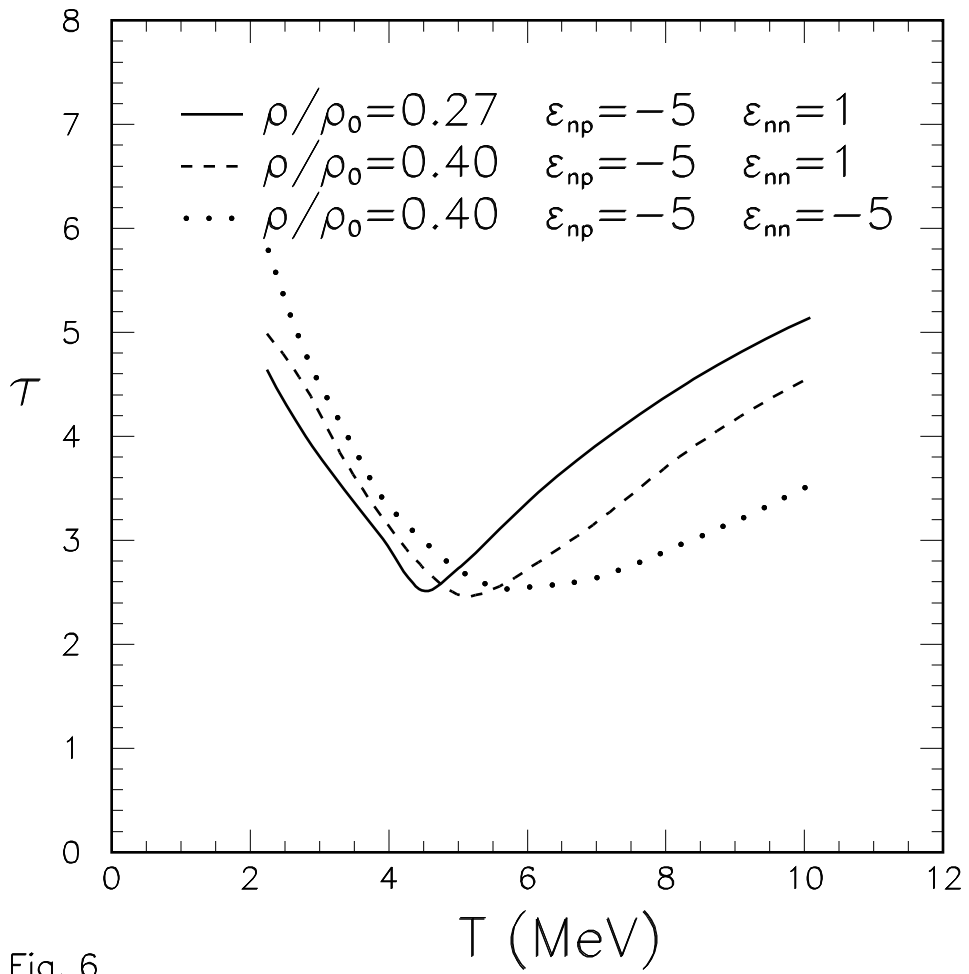


Fig. 6

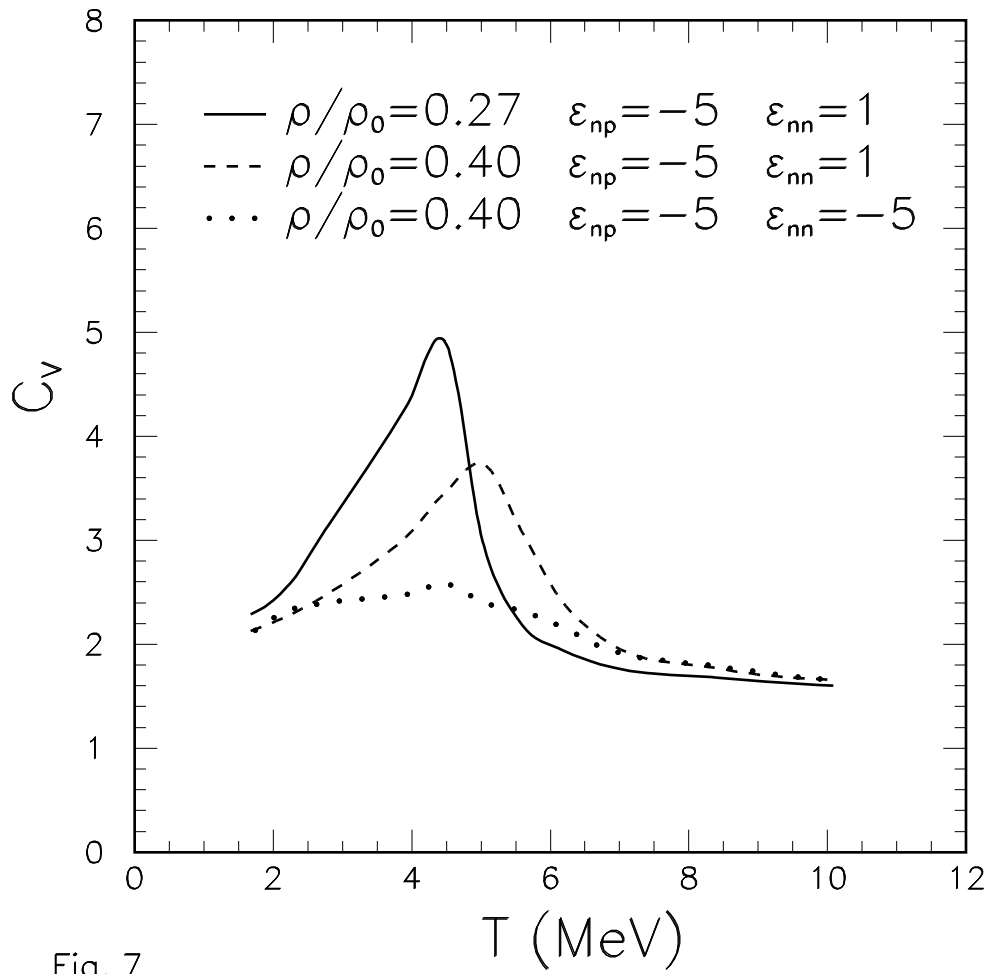


Fig. 7

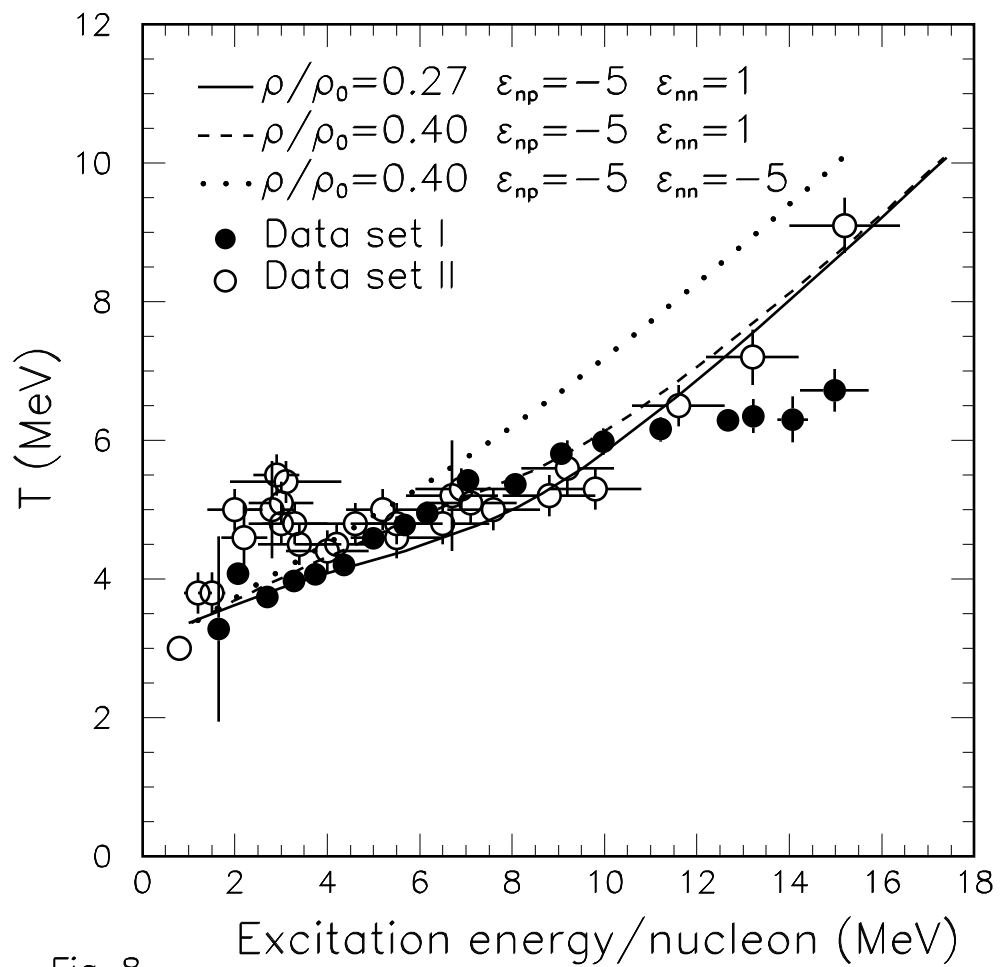


Fig. 8

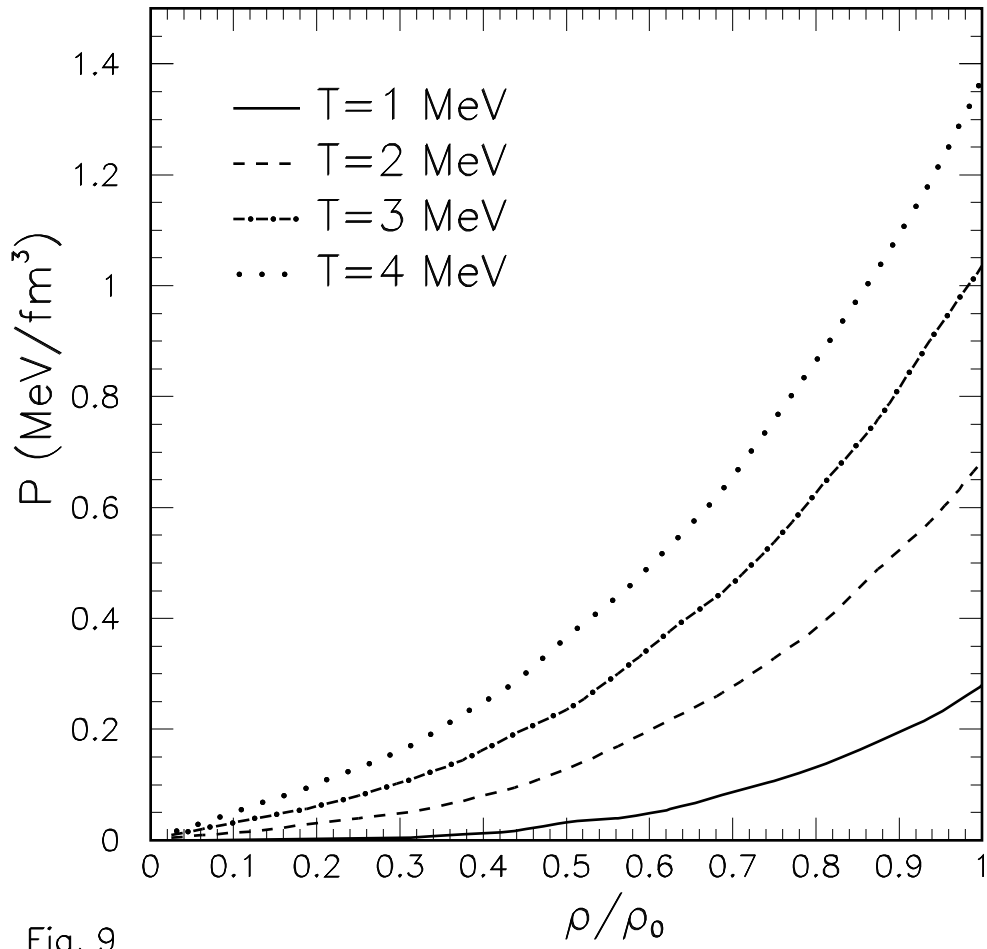


Fig. 9

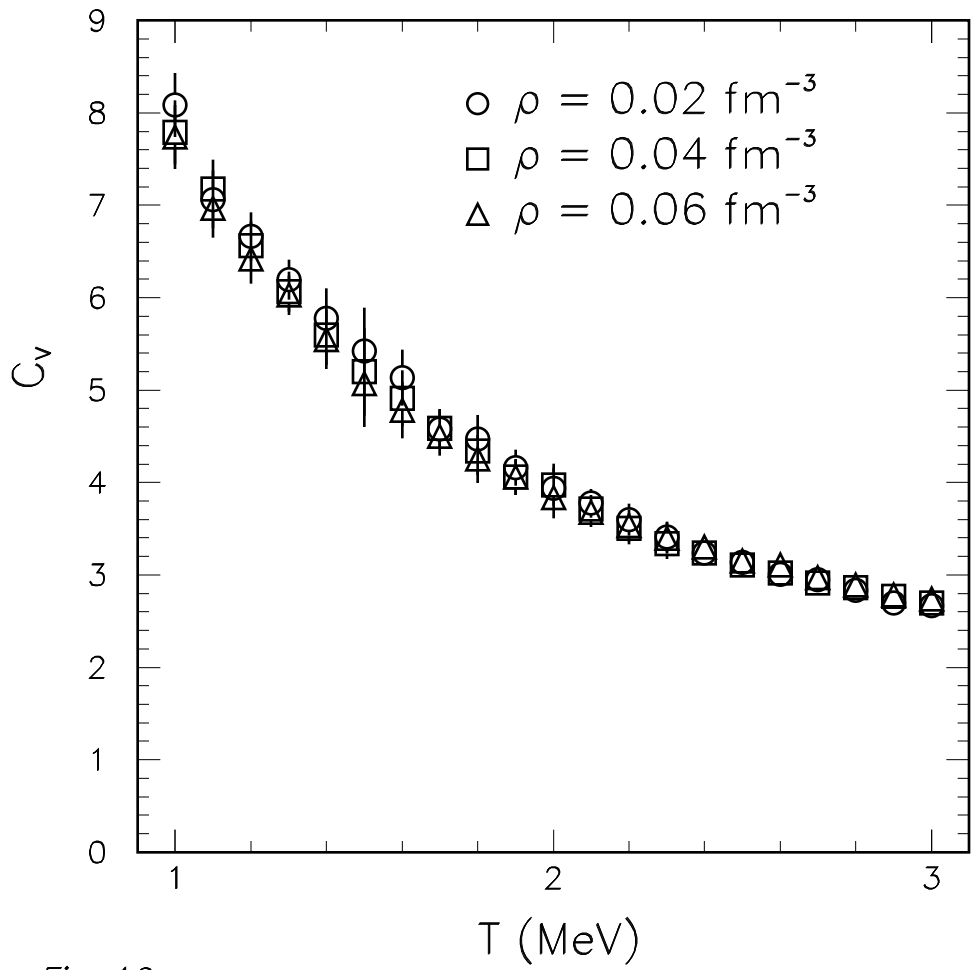


Fig. 10